CHAPTER IV
RESULTS AND DISCUSSION

4.1 Characterization

4.1.1 Mineral Purity

XRD was used to assess the mineral purity of clinoptilolite. It was found that the purity of clinoptilolite in this study was > 90%.

4.1.2 Surface Area and Pore Volume

Using the BET surface analyzer, the surface area and pore volume of clinoptilolite were determined to be 31.89 m^2/g and 0.0064 cm^3/g, respectively.

4.2 Ammonium Adsorption and Desorption

4.2.1 Ammonium Adsorption Isotherm

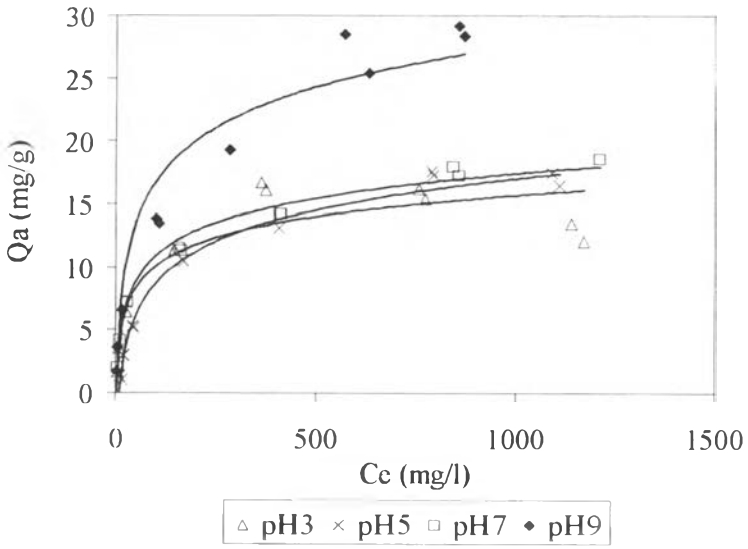

Figure 4.1 Adsorption isotherms of NH_4^+ on natural clinoptilolite at various pH conditions.

Adsorption isotherms of NH_4^+ on clinoptilolite at various pH conditions are shown in Figure 4.1. It can be seen from this figure that the maximum adsorption

capacities were in a range of 20-30 mg NH_4^+/g clinoptilolite. When comparing the adsorption among various pH values studied, it was found that amount of ammonium adsorbed increased with increasing pH. This is attributed to the increase in the number of sorption sites available on the clinoptilolite surface and the decrease of competing ions (H^-) for these sites as pH increased.

4.2.2 Kinetics of Ammonium Adsorption

Figures 4.2 and 4.3 show the kinetics of NH_4^+ adsorption on clinoptilolite at different pH conditions in terms of concentration in liquid phase (C_t) and solid phase (Qa_t), respectively. It can be seen from both figures that NH_4^+ ions were adsorbed rapidly during the first 10 min, then the adsorption gradually slowed down, and reached equilibrium within approximately 100 min. In addition, the extent of adsorption as indicated by a reduction in C_t or an increase in Qa_t was found to be highest at pH 9. This is in good agreement with the results observed in the previous section (Figure 4.1). Table 4.1 shows the initial rate of adsorption (k_a) of NH_4^+ on natural clinoptilolite at various pH conditions. As expected, the initial rate of NH_4^+ adsorption increased with increasing pH.

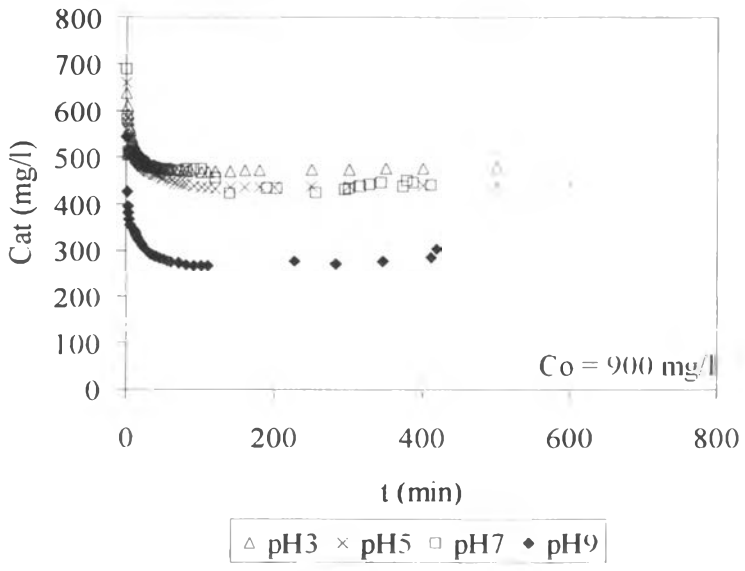

Figure 4.2 Liquid phase concentration of NH_4^+ (Ca_t) during adsorption on clinoptilolite at various pH conditions as a function of time.

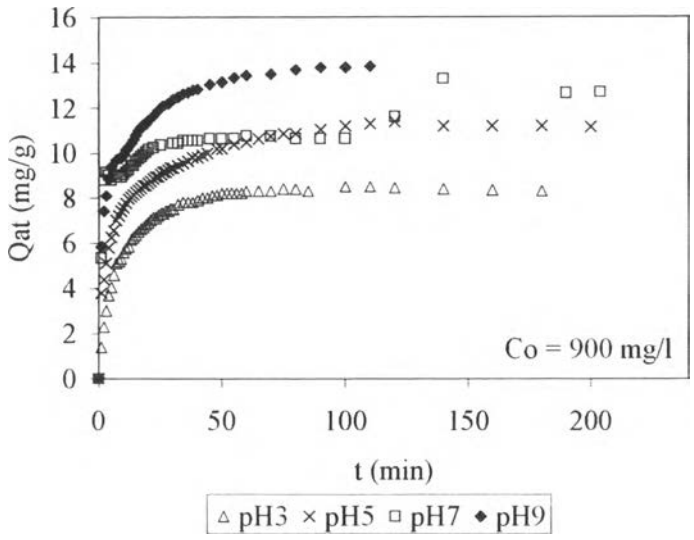

Figure 4.3 Solid phase concentration of NH_4^+ (Qa_t) during adsorption on clinoptilolite at various pH conditions as a function of time.

Table 4.1 Initial rate of adsorption (k_i) of NH_4^+ on natural clinoptilolite at various pH conditions

pH	k_i (mg NH_4^+/mg clinoptilolite min)
3	0.81
5	1.22
7	1.77
9	2.31

The experimental data obtained from the kinetic study were fitted with various kinetic models including zeroth order, first order, second order, parabolic diffusion, Elovich, and power function model. To evaluate the goodness of fit of the equations, the linear coefficient of determination (r^2) and the standard error (SE) of the estimate would be compared. This SE was calculated according to the equation:

$$SE = [\Sigma(X_t - X_t^*)^2 / n\text{-}2]^{1/2} \quad (4.1)$$

where X_t and X_t^* represent the amount of ion measure and calculated at time t respectively, and n is the number of measurement points.

A relatively high r^2 value and low SE indicated the goodness of conformity between experimental data and the model-predicted values. These meant a model successfully described the kinetics of nutrient adsorption and desorption by clinoptilolite. However, it should be noted that a model could not be used to definitively determine the mechanisms of ion adsorption and desorption (Kithome *et al.*, 1998).

Table 4.2 shows the linear coefficient of determination (r^2) and the standard error (SE) of the estimate for NH_4^+ adsorption on natural clinoptilolite at various pH conditions. The adsorption data were found to conform to the Elovich model, with acceptable r^2 values (> 0.99) and relatively low SE values, except for pH 7. This model describes that a number of different processes may be involved in the adsorption such as bulk and surface diffusion, activation and inactivation of the surfaces. The model has previously been used to describe the kinetics of ion adsorption and desorption on soils and soil minerals (Sparks and Jardine, 1984; Peryea *et al.* 1985). It has recently been used to model ion adsorption on natural zeolite by Kithome *et al.* (1998). The plots showing kinetic data of NH_4^+ adsorption fitted with the Elovich model are shown in Figure 4.4 for a constant initial concentration and different pH values.

Table 4.2 Linear coefficient of determination (r^2) and standard error (SE) of estimates obtained from various kinetic models for the adsorption of NH_4^+ on natural clinoptilolite at various pH conditions

Model	pH 3		pH 5		pH 7		pH 9	
	r^2	SE	r^2	SE	r^2	SE	r^2	SE
Zero order	0.707	4.103	0.609	6.685	0.266	8.963	0.591	8.292
First order	0.966	0.208	0.799	0.420	-3.248	0.916	0.864	0.419
Second order	0.340	0.181	0.454	0.067	0.275	0.036	0.585	0.046
Parabolic	0.897	0.076	0.830	0.078	.0.460	0.115	0.807	0.088
Elovich	**0.992**	**0.152**	**0.996**	**0.107**	**0.812**	**0.467**	**0.990**	**0.180**
Power function	0.921	0.104	0.965	0.044	0.725	0.068	0.978	0.028

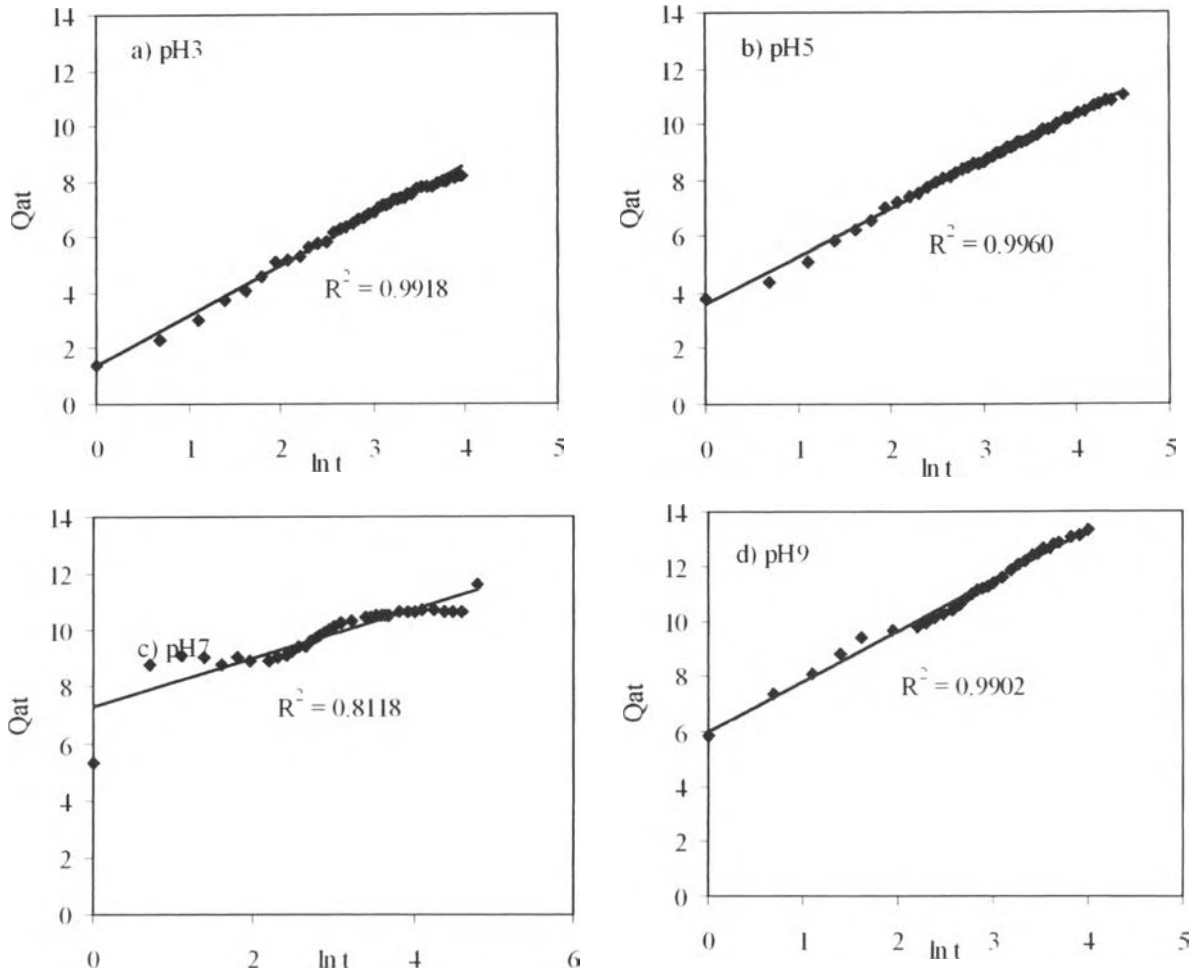

Figure 4.4 Kinetics of NH_4^+ adsorption on clinoptilolite at various pH conditions described by Elovich model.

Nevertheless, Wu *et al.* (2000) reported that the plot of fractional ion adsorbed (Fa) as a function of $t^{1/2}$ may present a multi-linearity, which indicates that two or more steps occur. On the other hand, the plot between Fa versus $t^{1/2}$ indicated intraparticle diffusion. Figure 4.5 shows the plot of fractional NH_4^+ ion adsorbed (Fa) at pH 9 as a function of $t^{1/2}$. The first, sharper portion indicated the external surface adsorption or instantaneous adsorption stage. The second portion was the gradual adsorption stage, where the intraparticle diffusion control took place. The third portion was final equilibrium stage where the intraparticle diffusion started to slow down to extremely low solute concentrations in the solution. Good r^2 of data in this model justifies the adsorption mechanisms.

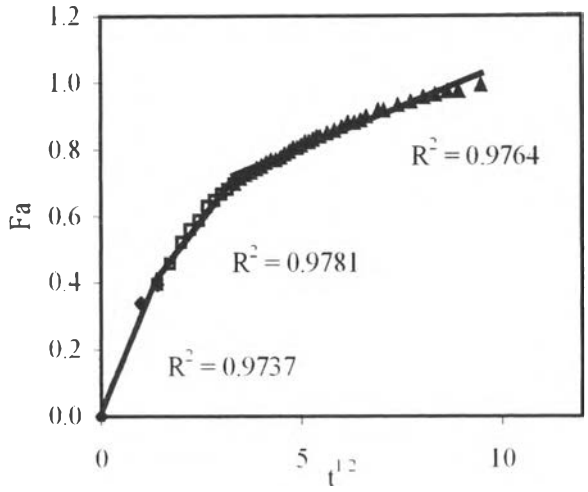

Figure 4.5 The plot of fractional NH_4^+ ion adsorbed (Fa) as a function of $t^{1/2}$ (pH 9).

Table 4.3 show the slope of the line in each stage, which was termed as the rate parameter $k_{ap,i}$ (i = 1-3) (Wu *et al.*, 2000). When comparing among three stages, the first stage, having the highest rate parameters ranging from 0.2080–0.4060, was the fastest diffusion process. It was also found that the external surface adsorption rate increased with increasing pH. After the first stage, the stage of intraparticle diffusion, with $k_{ap,2}$ in the range of 0.0866-0.1629, took place and extended to about 60 min, then the diffusion rate started to decrease upon entering the third stage of adsorption (equilibrium).

Table 4.3 The rate parameter $k_{ap,i}$ (i = 1-3) of kinetics of NH_4^+ adsorption on clinoptilolite at various pH conditions obtained from the plot of fractional ion adsorbed (Fa) as a function of $t^{1/2}$

Stage	$k_{ap,i}$ ($min^{-1/2}$)			
	pH 3	pH 5	pH 7	pH 9
1	0.21	0.30	0.38	0.41
2	0.16	0.16	0.05	0.09
3	0.06	0.05	0.01	0.04

4.2.3 Ammonium Desorption

In this part of the study, clinoptilolite samples after the adsorption cycle were subjected to a desorption process by using various cations to exchange with the adsorbed NH_4^+. Clinoptilolite with different adsorbed amount of NH_4^+ from the adsorption experiments conducted at pH 9 were chosen for the desorption study. In the attempt to desorb the NH_4^+ adsorbed on clinoptilolite, NaCl was first used as a desorbent in the study at various concentrations. Figure 4 6 shows desorption of ammonium ions adsorbed on natural clinoptilolite at various concentrations of NaCl.

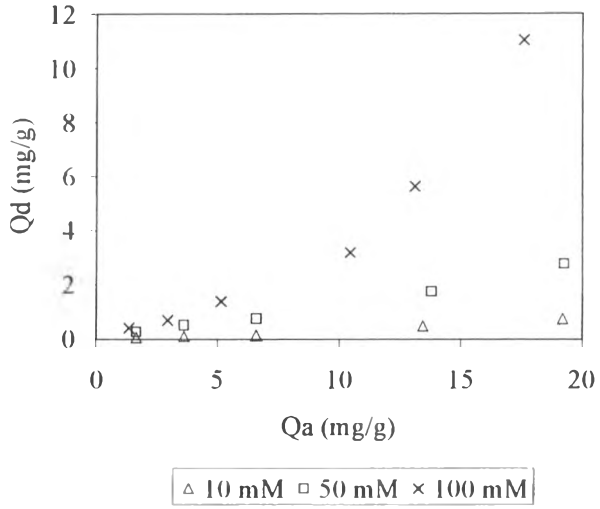

Figure 4.6 Desorption of ammonium ions adsorbed on natural clinoptilolite at various concentrations of NaCl.

From Figure 4 6, it can be seen that a gradual increase in the desorbed amount of sorbed NH_4^+ was observed with increasing NaCl concentration. At NaCl concentration of 50 mM, approximately 10% of NH_4^+ initially adsorbed on clinoptilolite could be desorbed whereas when 100 mM NaCl was used the desorbed amount increased to as high as 60% of the adsorbed amount. It should be noted that the desorbed amount (Q_d) was found to be very small when the adsorbed amount (Q_a) was less than 5 mg/g. Beyond that, the desorbed amount significantly increased with increasing amount of NH_4^+ adsorbed on clinoptilolite. This can be explained by the fact that when the adsorbed amount (Q_{ads}) was less than 5 mg/g, clinoptilolite surface was only partially covered by NH_4^+ ions. Therefore, Na^+ ions can get

adsorbed on the vacant sites on clinoptilolite surface without having to exchange with adsorbed NH_4^+, resulting in a small amount of NH_4^+ desorbed from clinoptilolite as seen in Figure 4.6.

The next set of experiments in this part of the study was carried out to examine the effect of type of cation on the desorption of NH_4^+ adsorbed on clinoptilolite. Two types of cations Ca^{2+} and Na^+, in form of $CaCl_2$ and NaCl, respectively, were used. In this comparative study, the salt concentration was fixed at 100 mM for all types of salt. The effect of salt type on the desorption of NH_4^+ adsorbed on clinoptilolite is shown in Figure 4.7. It can be seen that $CaCl_2$ had slightly greater effect on the desorbed amount of NH_4^+ than NaCl did. This could be explained that for some easily accessible sites a single Ca^{2+} ion may replace more than one NH_4^+ ions whereas Na^+ ion can replace only one NH_4^+ sorbed on clinoptilolite.

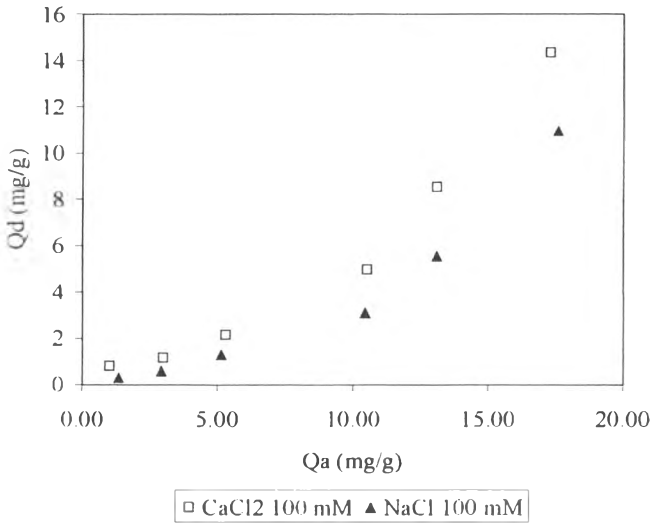

Figure 4.7 Desorption of ammonium ion adsorbed on natural clinoptilolite with different types of salt in the solution.

4.2.4 Kinetics of Ammonium Desorption

Figures 4.8 and 4.9 show the kinetics of NH_4^+ desorption from clinoptilolite in terms of NH_4^+ concentration in bulk liquid phase (C_t) and solid phase (Qi_t), respectively. This experiment was carried out at pH 9 and $CaCl_2$ with the concentration of 1000 mM. Similarly to the adsorption part, NH_4^+ ions were desorbed rapidly, then the desorption gradually slowed down until it reached equilibrium. However, the initial rate of desorption (k_d) of NH_4^+ from natural clinoptilolite at the same pH condition was found to be much higher than that of the adsorption part . This was probably due to the Ca^{2+} displacing ion in the solution of the desorption system

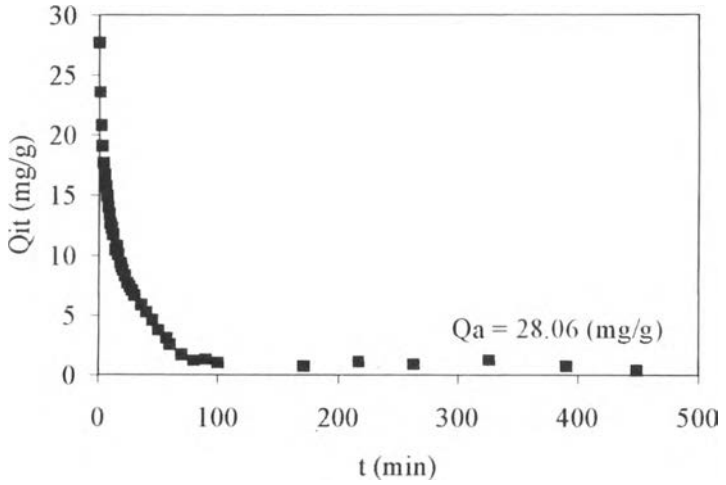

Figure 4.8 Liquid phase concentration of NH_4^+ (Cd_t) during desorption from clinoptilolite at pH 9 with initial amount adsorbed NH_4^+ of 28.06 mg NH_4^+/g CL using $CaCl_2$ 1000 mM.

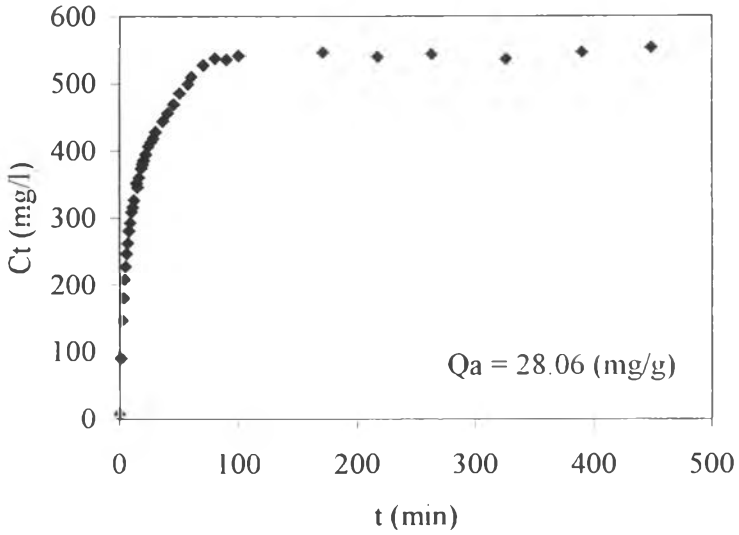

Figure 4.9 Solid phase concentration of NH_4^+ (Qd_t) during desorption from clinoptilolite at pH 9 with initial amount adsorbed NH_4^+ of 28.06 mg NH_4^+/g CL using $CaCl_2$ 1000 mM.

The same analysis used in the adsorption part can be applied to the data obtained in the desorption study. The desorption kinetic data were fitted with the same set of kinetic models used in the previous part. The linear coefficient of determination (r^2) and the standard error (SE) of the estimate for NH_4^+ desorption from natural clinoptilolite are shown in Table 4.4. Again, the Elovich model was found to best describe the NH_4^+ desorption, suggesting that several processes such as bulk and surface diffusion, and surface activation/inactivation were involved in NH_4^+ desorption.

Figure 4.10 shows the plot of fractional NH_4^+ ion desorbed (Fd) versus $t^{1/2}$ from the kinetic data of the desorption of NH_4^+ on clinoptilolite at pH. The first stage, which was the external surface desorption, was completed within 1 min, then the second stage, stage of intraparticle diffusion, attained and extended to about 15 min. The slope of the line in each stage, which was termed as the rate parameter $k_{dp,i}$ (i = 1-3) were listed in Table 4.5. It was seen that the desorption rate of these two stages were much faster than the last rate of the last stage. After that the intraparticle started to slow down due to the high NH_4^+ concentration in the solution.

Table 4.4 Linear coefficient of determination (r^2) and standard error (SE) of estimates for NH_4^+ obtained from various kinetic models for the desorption of NH_4^+ from natural clinoptilolite.

Model	r^2	SE
Zero order	0.738	11.969
First order	0.863	0.270
Second order	0.841	0.073
Parabolic	0.923	0.060
Elovich	**0.997**	**0.331**
Power function	0.958	0.078

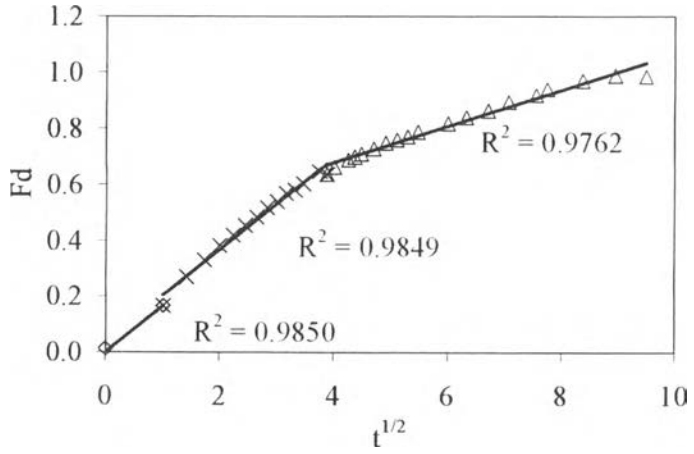

Figure 4.10 The plot of fractional NH_4^+ ion desorbed (Fd) as a function of $t^{1/2}$ (pH 9).

Table 4.5 The rate parameter $k_{dp,i}$ (i = 1-3) of kinetics of NH_4^+ desorption from clinoptilolite at pH 9 obtained from the plot of fractional ion adsorbed (Fa) as a function of $t^{1/2}$

Stage	$k_{dp,i}$ ($min^{-1/2}$)
1	0.17
2	0.16
3	0.06

4.3 Potassium Adsorption and Desorption

4.3.1 Potassium Adsorption Isotherm

Adsorption isotherms of K^+ on clinoptilolite at various pH conditions are shown in Figure 4.11. However, all of the experiments of potassium ion that conducted at pH 9 were omitted because it was suspected that the formation of KOH might start to occur at this high pH. This may lower the availability of K^+ ions for adsorption. The results were very similar to the NH_4^+ adsorption discussed in the previous section. However, it can be obviously seen that K^+ ions were adsorbed on clinoptilolite to a much greater extent as compared to NH_4^+ ions. Clinoptilolite has been shown to adsorb as high as 60 mg of K^+ per gram of clinoptilolite (at pH 7). When comparing the adsorption at various pH values, the general trend was observed that the adsorption of K^+ was higher at higher pH.

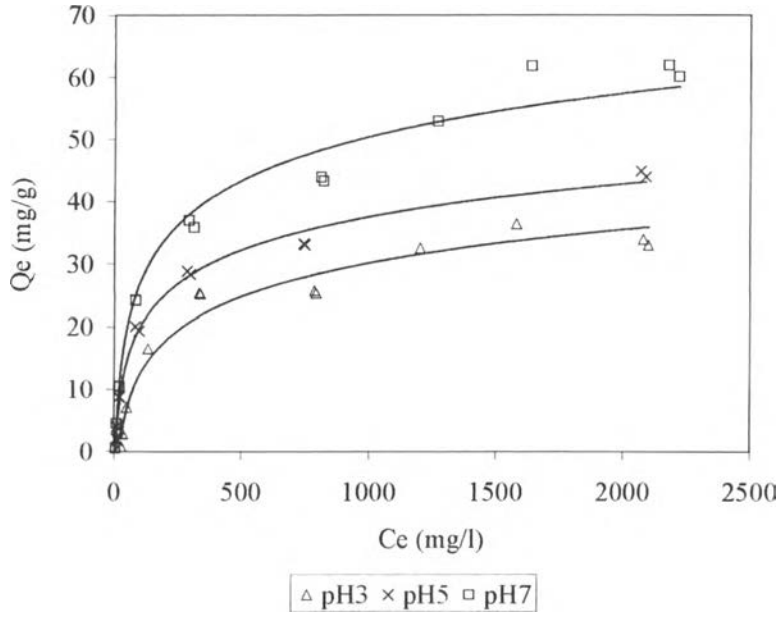

Figure 4.11 Adsorption isotherms of K^+ on clinoptilolite at various pH conditions.

4.3.2 Kinetics of Potassium Adsorption

Figures 4.12 and 4.13 show the kinetics of K^+ adsorption on clinoptilolite at different pH conditions in terms of concentration in liquid phase (C_t) and solid phase (Qa_t), respectively. Similar to NH_4^+ adsorption (Figure 4.2 and

Figure 4.3), it can be seen from both figures that K^+ ions were adsorbed rapidly during the first 10 min, then the adsorption gradually slowed down, and reached equilibrium within approximately 100 min after the beginning of the adsorption.

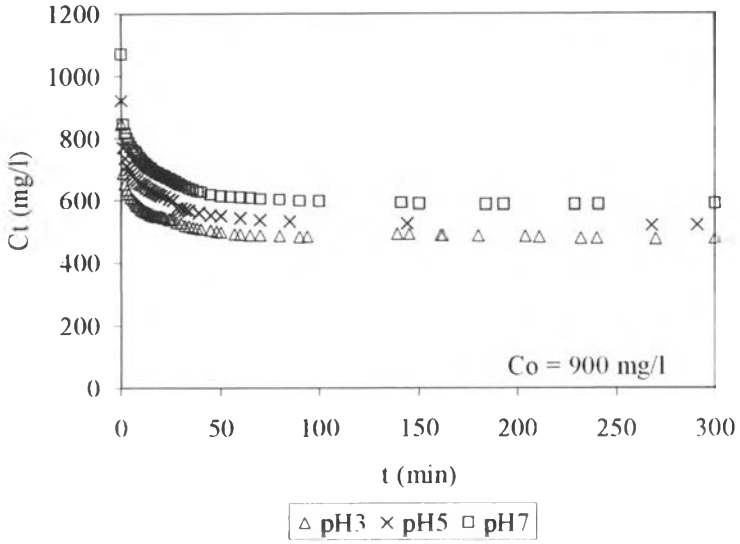

Figure 4.12 Liquid phase concentration of K^+ (Ca_t) during adsorption on clinoptilolite at various pH conditions as a function of time.

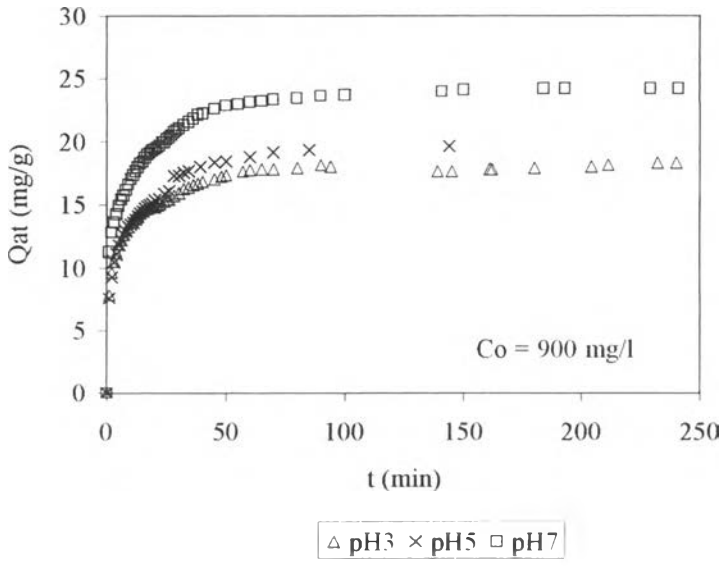

Figure 4.13 Solid phase concentration of K^+ (Qa_t) during adsorption on clinoptilolite at various pH conditions as a function of time.

The initial rates of adsorption (k_i) of K+ on natural clinoptilolite at various pH conditions were shown in Table 4.6. The highest value of k_i was observed at pH 7.

Table 4.6 Initial rate of adsorption (k_i) of K^+ on natural clinoptilolite at various pH conditions

pH	k_a (mg K^+/mg clinoptilolite min)
3	3.46
5	4.11
7	4.49

The experimental data obtained from the kinetic study were fitted with various kinetic models, which were zero order, first order, second order, parabolic diffusion, Elovich, and power function model. The linear coefficient of determination (r^2) and the standard error (SE) of the estimate for K+ adsorption on natural clinoptilolite at various pH conditions are shown in Table 4.7. Similar to NH_4^+ adsorption, the K^+ adsorption data were found to conform to the Elovich model, with acceptable r^2 values (> 0.98) and SE value. The K^+ adsorption data were also well fitted with the power function model, which indicated diffusion controlled (Allen *et al.*, 1995). The power function model has previously been used to describe the kinetics of ion adsorption and desorption on soils and soil minerals (Allen *et al.*, 1995; Galadima and Silvertooth, 1998; Sanjay and Chahal, 2002, Alireza and Mahmoud, 2002). The plots showing K^+ adsorption fitted with Elovich model are shown in Figure 4.14 for a constant initial concentration and different pH values.

Figure 4.15 shows the plot of fractional K^+ ion adsorbed (Fa) versus $t^{1/2}$ from the kinetic data of the K^+ adsorption on clinoptilolite at pH 3. The slope of the line in each stage is listed in Table 4.8. When comparing among three stages, the first stage, with the rate parameter ranging from 0.3562-0.4061, was the fastest diffusion process. It was found that the external surface adsorption rate increased with increasing pH. After the first stage, the stage of intraparticle diffusion, with

$k_{ap,2}$ in the range of 0.0893-0.1459, and the third stage of adsorption took place, respectively.

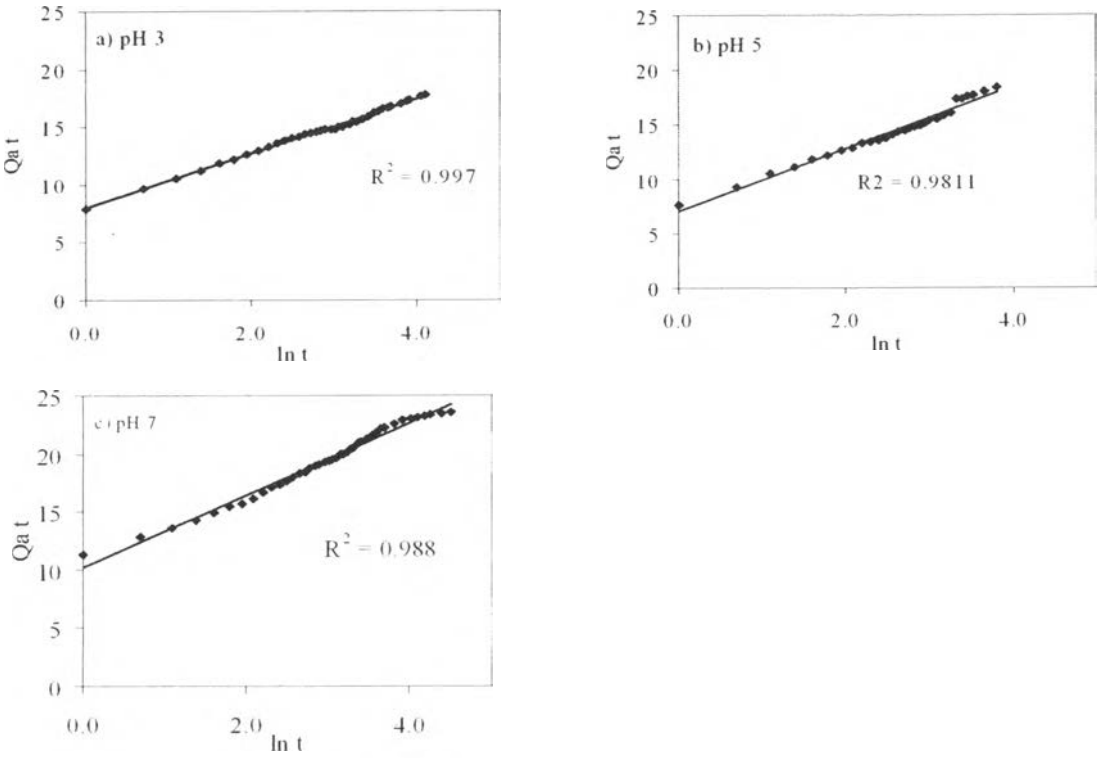

Figure 4.14 Kinetics of K_4^+ adsorption on clinoptilolite at various pH conditions described by Elovich model.

Table 4.7 Linear coefficient of determination (r^2) and standard error (SE) of estimates obtained from various kinetic models for the adsorption of K+ on natural clinoptilolite at various pH conditions

Model	pH 3		pH 5		pH 7	
	r^2	SE	r^2	SE	r^2	SE
Zero order	0.575	11.34	0.674	10.161	0.555	463
First order	0.654	0.478	0.719	22.243	0.610	0.774
Second order	0.572	0.034	0.651	0.044	0.580	0.022
Parabolic	0.788	0.084	0.871	0.069	0.786	0.075
Elovich	**0.997**	**0.130**	**0.981**	**0.369**	**0.988**	**0.328**
Power function	**0.981**	**0.024**	**0.991**	**0.020**	**0.990**	**0.016**

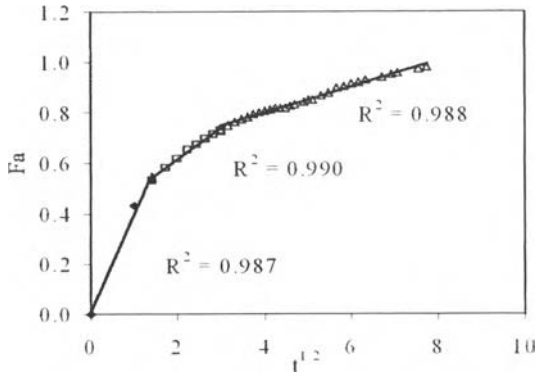

Figure 4.15 The plot of fractional K^+ ion adsorbed (Fa) as a function of $t^{1/2}$ (pH 3).

Table 4.8 The rate parameter $k_{ap,i}$ (i = 1-3) of kinetics of K^+ adsorption on clinoptilolite obtained from the plot of fractional K^+ ion adsorbed (Fa) at pH 3 as a function of $t^{1/2}$

Stage	$k_{ap,i}$ ($min^{-1/2}$)		
	pH 3	pH 5	pH 7
1	0.40	0.360	0.41
2	0.12	0.13	0.09
3	0.05	0.08	0.04

4.3.3 Potassium Desorption

Similar to NH_4^+, the same treatment can be applied to K^+. Following the adsorption of K^+, clinoptilolite was subject to desorption by using cations, Na^+ to exchange with the adsorbed K^+. Clinoptilolite with different adsorbed amount of K^+ from the adsorption experiments conducted at pH 7 were chosen for the desorption study.

In this part of the study, NaCl was first used as a desorbent in the study at various concentration as shown in Figure 4.16. It can be seen that a gradual increase in the desorbed amount of sorbed K^+ was observed with increasing NaCl concentration. At NaCl concentration of 100 mM, approximately 40% of sorbed K^+ on clinoptilolite could be desorbed whereas at 500 mM the desorbed amount corresponding to 50% of the adsorbed amount was observed. The desorbed amount

of K^+ could be observed as high as 85% of total adsorbed when NaCl concentration was 1000 mM. Moreover, the desorbed amount increased with increasing amount of K^+ adsorbed on clinoptilolite. The explanation was quite similar to the adsorption. The partially adsorbed of K^+ on clinoptilolite surface, thus Na^+ ions can be adsorbed on the vacant sites on the surface without exchanging with adsorbed K^+, causing a small amount of K^+ desorbed.

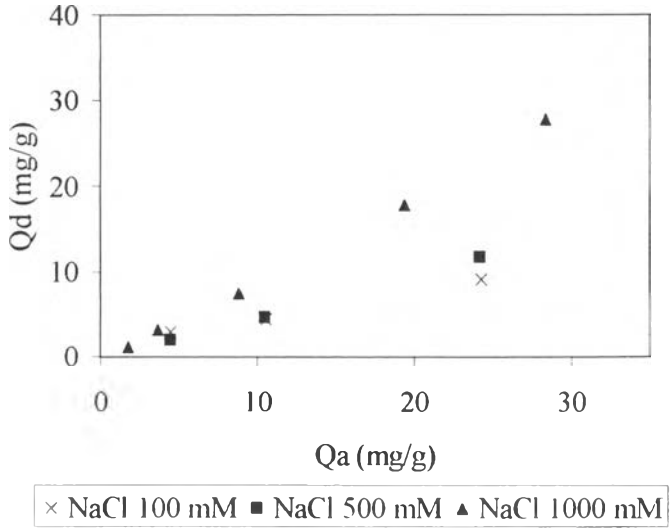

Figure 4.16 Desorption of potassium ions adsorbed on natural clinoptilolite at various concentrations of NaCl.

In the next part of the experiment, NaCl and $CaCl_2$ at the same molar concentration (1000 mM) were used to desorb K^+ adsorbed on clinoptilolite. The desorbed amount of K^+ at different amount of K^+ initially adsorbed on clinoptilolite by these two cations are shown in Figure 4.17.

From the results, it can be seen that, at this high concentration of salt (1000 mM), the desorbed amount of K ions initially adsorbed on clinoptilolite could be seen even at low surface adsorption (e.g., Qa less than 10 mg/g). For both types of cations, the higher desorbed amount of K^+ (Q_d) was observed at higher amount of K^+ initially loaded on clinoptilolite (Qa). As high as 85% of K^+ initially adsorbed on clinoptilolite could be desorbed when clinoptilolite was fully loaded with K^+ (e.g.,

when Qa > 25 mg/g). In addition, it can be seen that, regardless of the type of cation used, the amount of K^+ desorbed from clinoptilolite was quite similar.

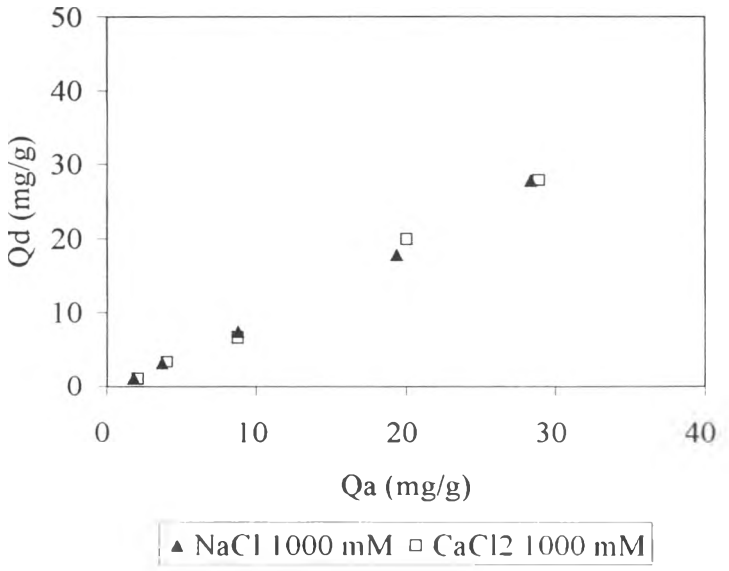

Figure 4.17 Desorption of adsorbed potassium ions on natural clinoptilolite by two types of cations.

4.3.4 Kinetics of Potassium Desorption

Figures 4.18 and 4.19 show the kinetics of K^+ desorption from clinoptilolite in terms of concentration in liquid phase (C_t) and solid phase (Qi_t), respectively. This experiment was carried out at pH 7 and $CaCl_2$ with the concentration of 1000 mM. The result observed was quite similar to the adsorption part, K^+ ions were desorbed rapidly, then the desorption gradually slowed down and reached equilibrium eventually. However, the initial rate of desorption (k_d) of K^+ from natural clinoptilolite at the same pH condition was found to be much higher than that of the adsorption part. It was suspected that the Ca^{2+} ions in the system had strongly effect to the desorption of K^+.

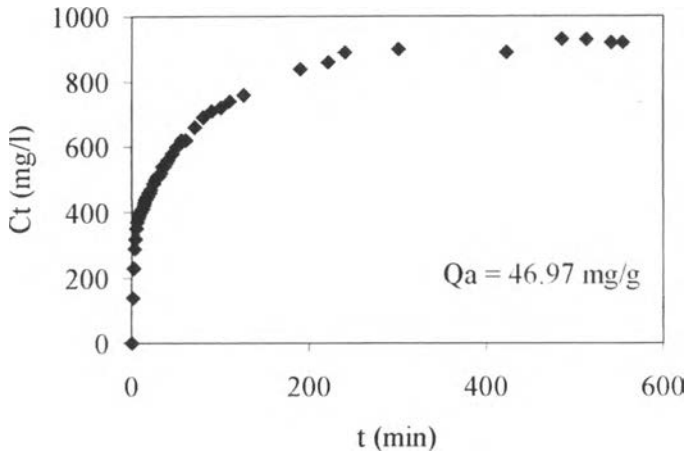

Figure 4.18 Liquid phase concentration of K^+ (Cd_t) during desorption from clinoptilolite at pH 7 with initial amount adsorbed K^+ of 46.97 mg K^+/g CL using $CaCl_2$ 1000 mM.

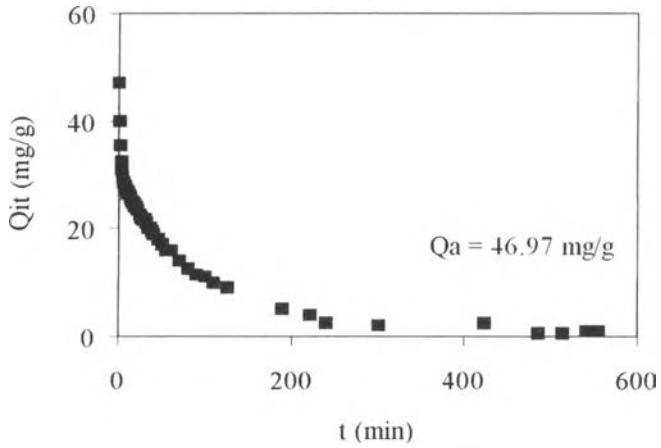

Figure 4.19 Solid phase concentration of K^+ (Qd_t) during desorption from clinoptilolite at pH 7 with initial amount adsorbed K^+ of 46.97 mg K^+/g CL using $CaCl_2$ 1000 mM.

The kinetic experimental data were fitted with the same kinetic models as in the previous kinetic part. The linear coefficient of determination (r^2) and the standard error (SE) of the estimate for K^+ desorption from natural clinoptilolite are shown in table 4.9. The experimental data was found to conform to

Elovich and the power function model, with acceptable r^2 and SE value. In addition, the experimental data were also well fitted with the plot of fractional NH_4^+ ion desorbed (Fd) at pH 7 as a function of $t^{1/2}$ (Figure 4.20).

Table 4.9 Linear coefficient of determination (r^2) and standard error (SE) of estimates for K^+ obtained from various kinetic models for the desorption of K^+ from natural clinoptilolite

Model	r^2	SE
Zero order	0.454	46.697
First order	0.288	0.726
Second order	0.963	0.017
Parabolic	0.647	0.085
Elovich	**0.972**	**1.072**
Power function	**0.983**	**0.016**

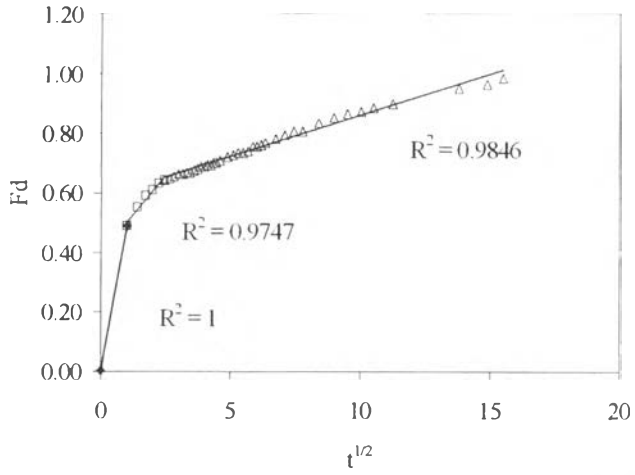

Figure 4.20 The plot of fractional K^+ ion desorbed (Fd) as a function of $t^{1/2}$ (pH 7).

Table 4.10 shows the slope of the line in each stage ($k_{dp,i}$, where i = 1-3). The first stage, which was the external surface desorption, was completed within 1 min, then the second stage, stage of intraparticle diffusion, attained and extended to about 6 min. After that the intraparticle started to slow down due to the high K^+ concentration in the solution.

Table 4.10 The rate parameter $k_{dp,i}$ (i = 1-3) of kinetics of K^+ desorption from clinoptilolite obtained from the plot of fractional K^+ ion desorbed (Fd) at pH 7 as a function of $t^{1/2}$

Stage	$k_{dp,I}$ ($min^{-1/2}$)
1	0.49
2	0.10
3	0.03

4.4 Release of NH_4^+ and K^+ from Preloaded Clinoptilolite with Mixed-Nutrients

In this part of the experiment, the natural clinoptilolite was first loaded with predetermined concentration of NH_4Cl in order to obtain the partial NH_4^+ coverage. Then, NH_4^+ loaded clinoptilolite was mixed with KCl at desired concentration. After that, clinoptilolite with NH_4^+ and K^+ loaded were subjected to a desorption process by using Ca^{2+} in the form of $CaCl_2$ with the concentration of 1000 mM to exchange with the adsorbed NH_4^+ and K^+. All of the experiments were carried out at pH 7. Figure 4.21 shows the ratio of NH_4^+ and K^+ loaded on clinoptilolite.

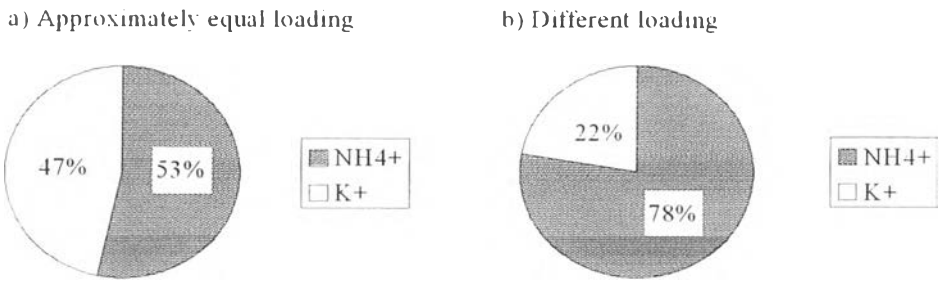

Figure 4.21 The ratio of NH_4^+ and K^+ loaded on natural clinoptilolite.

According to Figure 4.22 and Table 4.11, it was found that when two ions were approximately equal loaded on clinoptilolite (sample1), both NH_4^+ and K^+ ions released in approximately equal amount. However, when NH_4^+ and K^+ ions were loaded with different loading ratio (sample 2), K^+ ions tended to desorb in the much higher amount than that of the equal loading ratio. The reason might be the effect of NH_4^+ ions. When the concentration of NH_4^+ was much higher than K^+, the released NH_4^+ tended to replace K^+ ions that loaded on the clinoptilolite surface even though the selectivity of K^+ to clinoptilolite is higher than that of NH_4^+ to clinoptilolite. Similar phenomenon was also observed by Allen *et al.* (1995; 1996).

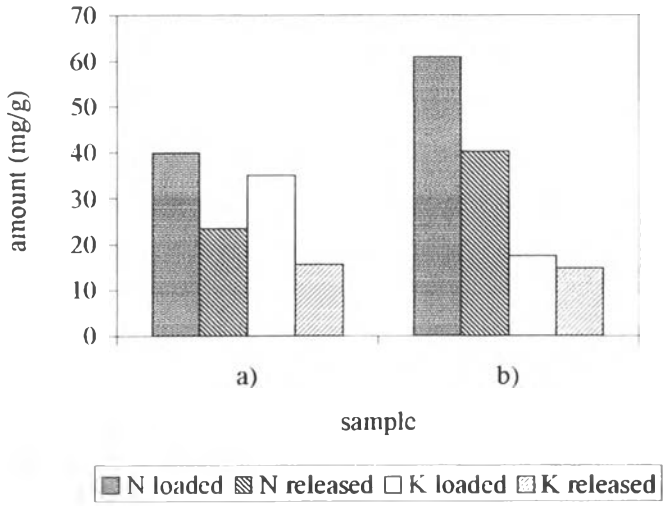

Figure 4.22 The amount of NH_4^+ and K^+ released compared to the amount of NH_4^+ and K^+ adsorbed.

Table 4.11 The percentage of ions loading on natural clinoptilolite and amount of ions released as percentage of original loading

Sample	Loading (%)		Release (% of original loading)	
	NH_4^+	K^+	NH_4^+	K^+
1	53.30	46.70	58.99	45.00
2	77.69	22.31	65.91	84.95